

Investigation of the Faraday Rotation Measure and Magnetic Field Structures of Several AGN Jets on Sub-Parsec to Parsec Scales

Shane P. O’Sullivan and Denise C. Gabuzda

Department of Physics, University College Cork, Cork, Ireland

Abstract. Preliminary VLBA polarisation results on 6 “blazars” from 6.5-cm to 7-mm are presented here. Observing at several different wavelengths, separated by short and long intervals, enabled reliable information about the magnetic (B) field structure to be obtained and for the effect of Faraday Rotation to be determined and corrected. For all sources the magnitude of the core Rotation Measure (RM) derived from the shorter wavelength data was greater than that derived from the longer wavelength data, consistent with a higher electron density and/or B-field strength closer to the central engine. A transverse RM gradient was detected in the jet of 0954+658, providing evidence for the presence of a helical B-field surrounding the jet. The RM in the core region of 2200+420 (BL Lac) displays sign changes in different wavelength intervals (on different spatial scales); we suggest an explanation for this in terms of modest bends in a helical B-field surrounding the jet.

1. Introduction

The Faraday effect causes a rotation of the plane of linear polarisation, described by: $\Delta\chi = RM\lambda^2$, with the rotation measure (RM) determined by the integral of the electron density and the dot product of the magnetic (B) field and the path length along the line of sight (LoS). A positive/negative RM indicates that the LoS B-field is pointing towards/away from the observer. $\Delta\chi$ is the change in the electric vector position angle (EVPA). Previous results indicated the presence of different RM signs in the core regions of 6 blazars in different wavelength intervals (O’Sullivan & Gabuzda 2006). This has two main possible origins: (1) the LoS B-field changes with distance from the centre of activity, or (2) since the previous observations were not simultaneous, it could be due to an intrinsic change in the overall jet B-field structure between observing epochs. Our new 8 wavelength observations are designed to test these possibilities.

2. Observations

Multi-wavelength (6.5, 5.9, 3.8, 3.4, 2.3, 1.9, 1.3 cm & 7 mm), simultaneous polarisation observations of 6 “blazars” (0954+658, 1156+295, 1418+546, 1749+096, 2007+777, 2200+420) were obtained on the VLBA over a 24-hr period on 2 July 2006. The calibration and imaging were done in AIPS using standard techniques. The integrated (Galactic) RMs were subtracted, to better isolate the RM distribution in the immediate vicinity of the AGNs (Pushkarev

2001 and references therein). Matched-resolution images were constructed for two separate wavelength intervals using the 5.9-cm beamsizes for the longer wavelength interval and the 1.9-cm beamsizes for the shorter wavelength interval. This was done to obtain more reliable information about the RM distribution and B-field in the long and short wavelength regimes, as can be seen from the plot of χ vs. λ^2 for 1156+295 for the whole wavelength range in Figure 1.

3. Rotation Measure Results

A summary of preliminary results is displayed in Table 1. Separate RMs were found for long and short wavelength intervals between which a clear transition was present (eg. Fig.1). The redshift, z , and the orientation of the jet EVPA relative to the jet direction (\parallel aligned, \perp orthogonal, $-$ no jet polarisation) are also given. For all sources the magnitude of the core RM is higher at shorter wavelengths, consistent with an increased electron number density closer to the central engine. A larger B-field strength can also contribute to this increase.

Table 1. Summary of RM results. All values in rad/m^2

Blazar	z	Jet EVPA vs. Jet Direction	Core RM (Long λ range)	Core RM (Short λ range)
0954 + 658	0.368	\parallel	-41 ± 14	-2207 ± 386
1156 + 295	0.729	\parallel	$+136 \pm 6$	$+1647 \pm 209$
1418 + 546	0.152	\perp	-65 ± 22	-483 ± 55
1749 + 096	0.320	$-$	-33 ± 24	-500 ± 347
2007 + 777	0.342	\parallel	$+636 \pm 110$	$+1946 \pm 140$
2200 + 420	0.069	\parallel	$+746 \pm 76 / -125 \pm 30$	-1144 ± 36

2200+420 (BL Lac) has quite a complicated and variable structure. The inner-jet has changed from a southwesterly direction in our 7 August 2002 observations (Gabuzda et al. 2006) to directly southwards in our current observations, consistent with the “precessing nozzle” proposed by Stirling et al. (2003). The RM map from 6.5-cm to 2.3-cm (Fig.2) shows a large positive value of $+746 rad/m^2$ at the northern end, which we consider to be the true core, since our spectral index map (corrected for the frequency dependent core shift; see Lobanov 1998) shows this region as being most optically thick; a negative RM of $-125 rad/m^2$ is observed just south of this region, while the rest of the jet has a low RM (essentially equal to zero within the errors) consistent with a much lower electron density in the vicinity of the optically thin jet. The RM map of 2200+420 from 7-mm to 1.9-cm (Fig.3) displays an RM of $-1144 rad/m^2$ in the core, which is larger in magnitude and different in sign than the observed northernmost RM for the longer wavelength data. The inner-jet RM has a smaller value of $-732 rad/m^2$; these regions probably correspond to the region of negative RM near the core in the longer wavelength RM map (Fig.2). An interesting feature in Fig.3 is the high, positive RM detected at the eastern edge

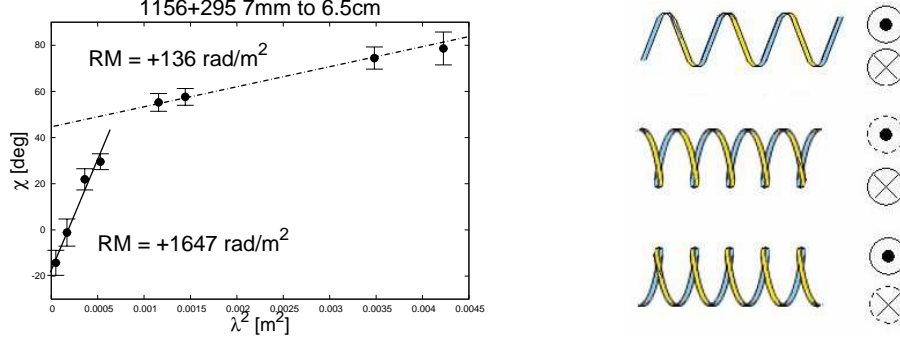


Figure 1. Left: Plot of χ vs. λ^2 for all observed wavelengths for 1156+295; the obvious increase in the slope at short wavelengths shows the need to split up the wavelength range to obtain more reliable information about the RM and B-field on different scales. Right: Helical field viewed: Side-on (top), Tail-on (middle), Head-on (bottom). Solid and dashed circles indicate the relative strength of the RM on the two sides of the jet. A black dot/cross indicates that the LoS B-field is pointing towards/away from us.

of the jet in the region where it bends, possibly indicating interaction with the surrounding medium.

The fact that the Faraday corrected polarisation vectors for 2200+420 from both frequency intervals (Fig.4) remain well aligned with the jet even as it goes through substantial bending can be understood if the implied transverse B-field represents the toroidal component of a helical field. 1418+546 is the only source in this sample with jet polarisation perpendicular to the jet direction (Table 1). This behaviour of the jet EVPAs is also natural if the jets have helical B-fields (Lyutikov et al. 2005), where polarisation perpendicular to the jet direction occurs when the poloidal component of the helical B-field dominates.

A transverse RM gradient was detected in the jet of 0954+658, which is a strong signature of the presence of a helical B-field surrounding the jet, confirmed by the results of Mahmud & Gabuzda 2007 (these proceedings).

4. Discussion

Our results for 2200+420 confirm the presence of an RM sign reversal in the core region. Since the dominant jet B-field is transverse to the jet and remains transverse while the jet bends, we will suppose a helical B-field surrounds the jet. The observed RM sign reversal can be explained by a slight bend of the jet, due, for example, to a collision with material in the parent galaxy or some instabilities inherent in the jet itself. (A longitudinal jet B-field with a change in the angle to the line of sight could also cause a RM sign reversal, but this does not correspond to the observed B-field.)

A side-on view of a helical B-field (Fig.1 Top right) will have a RM that will be equally strong on both sides of the jet, hence, a zero net RM will be observed for an unresolved jet. This would occur when the source is viewed at $1/\Gamma$ in the observer's frame. For a tail-on view of a helical B-field (ie. $\theta > 1/\Gamma$) (Fig.1 Middle), the dominant RM will be from the bottom half of the jet and a negative

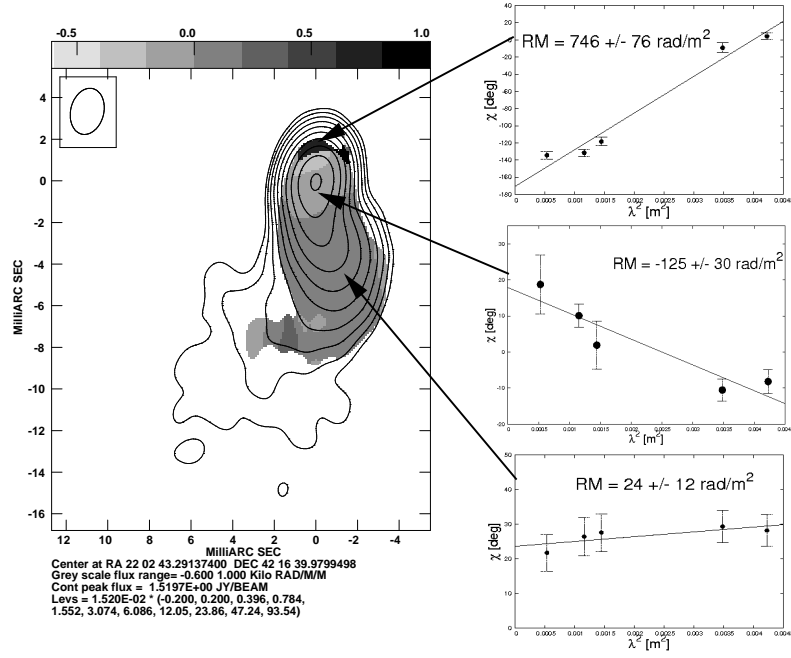


Figure 2. RM map for 2200+420 from 6.5-cm to 2.3-cm superimposed on the 5.9 cm I map. The accompanying plots are of χ vs. λ^2 for the indicated regions of the source.

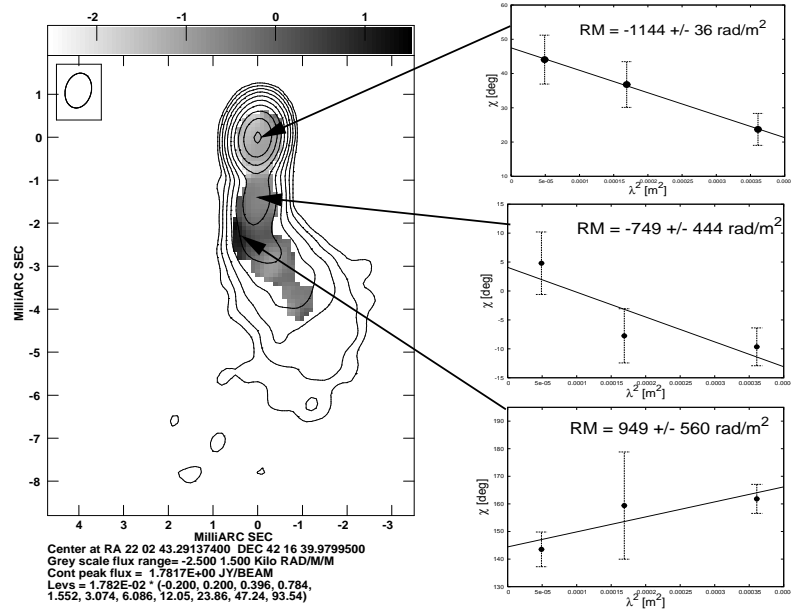


Figure 3. RM map for 2200+420 from 7-mm to 1.9-cm superimposed on the 1.9 cm I map. The accompanying plots are of χ vs. λ^2 for the indicated regions of the source.

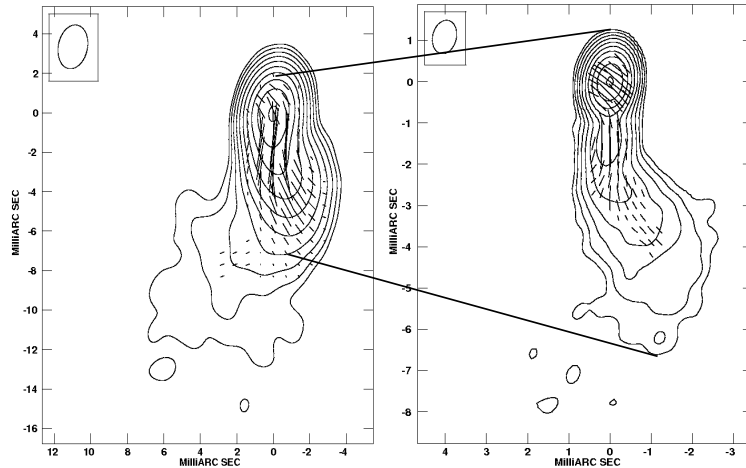


Figure 4. Left: 5.9 cm I map, Right: 1.9cm I map, for 2200+420; both with Faraday corrected EVPAs. Note alignment of jet EVPAs even as jet bends.

RM will be observed because the dominant LoS B-field will be pointing away from us. (Assuming the jet is not fully resolved in the transverse direction.) Conversely, for a head-on view of a helical B-field (ie. $\theta < 1/\Gamma$) (Fig.1 Bottom), a positive RM will be observed.

Therefore, regions with different RM signs in the jets of AGN can be explained within a helical B-field model as places where the jet is observed at angles greater than or less than $1/\Gamma$, due to bends in the jet. Since VLBI resolution is usually not sufficient to completely resolve the true optically thick core, the VLBI “core” consists of emission from the true core and some of the optically thin inner-jet. So if bends occur on scales smaller than the observed VLBI core, “core” RMs with different signs could be derived from observations at different wavelengths (ie. probing different scales of the inner-jet). In our future work, we will attempt to reconstruct the 3D path of the jet through space using the combined information from the observed distributions of the total intensity, linear polarisation, spectral index and rotation measure.

Acknowledgments. Funding for this research was provided by the Irish Research Council for Science, Engineering and Technology. The VLBA is a facility of the NRAO, operated by Associated Universities Inc. under cooperative agreement with the NSF.

References

- Gabuzda, D., Rastorgueva, E., Smith, P. & O’Sullivan, S. 2006, MNRAS, 369, 1596
- Lytikov, M., Pariev, V. I. & Gabuzda, D. C. 2005, MNRAS, 360, 869
- Lobanov, A. P. 1998, A&A, 330, 79
- Mahmud, M. & Gabuzda, D. C. 2007, these Proceedings
- O’Sullivan, S. P. & Gabuzda, D. C., 2006, Proceedings of the 8th EVN Symposium
- Pushkarev, A. B. 2001, Astron. Rep., 45, 667
- Stirling, A. M. et al. 2003, MNRAS, 341, 405